JPTM
http://journal.unnes.ac.id

FIRST MANDIBULAR MOLAR IMPLANT SYSTEM UNDER ORTHOTROPIC BONE VARIATIONS: A FINITE ELEMENT SENSITIVITY ANALYSIS

Fatkhu Amanulloh[1], Kriswanto[2], Ruben Bayu Kristiawan[3], Jamari[4], Athanasius Priharyoto Bayuseno[5], Dhiaulhaque[6], Dzikra Adi Pratama[7], Mohd Syahmi Jamaludin[8]

[1]Department of Mechanical Engineering Education, Faculty of Engineering, Universitas Negeri Semarang, Semarang, Central Java, Indonesia.
[2]Department of Mechanical Engineering, Faculty of Engineering, Universitas Diponegoro, Semarang, Central Java, Indonesia
[8]Department of Mechanical and Manufacturing, Faculty of Engineering, Universiti Malaysia Sarawak, Samarahan, Sarawak, Malaysia
Email: fatkhuamanulloh2@students.unnes.ac.id

Abstract

Physiological variability in bone mechanical properties may affect load transfer and biomechanical stability in dental implant systems. However, the influence of orthotropic elastic and shear properties on implant–bone biomechanics remains unclear. This study evaluated the sensitivity and robustness of a mandibular first molar implant system to variations in orthotropic bone properties using finite element analysis. A three-dimensional implant–bone model was analyzed under nine material configurations, including gradual orthotropic variations (±15% of baseline) and independent modifications of the elastic and shear modulus. Biomechanical responses were evaluated using von Mises stress, principal stresses, strains, and displacements. Stress concentrations were primarily located at the implant–abutment connection and crestal cortical bone, indicating the main load-transfer pathways. Increasing directional stiffness reduced peri-implant strain and displacement but increased cortical stress, revealing a trade-off between deformation reduction and local stress concentration. Elastic modulus predominantly influenced global stress redistribution, whereas shear modulus had a greater effect on local deformation and peri-implant stability. Strain and displacement were more sensitive to material variations than stress-based parameters. These findings emphasize the importance of orthotropic material representation for realistic biomechanical assessment of dental implant systems under physiological variations in bone quality.

Keywords: Dental implant; finite element analysis; orthotropic bone; sensitivity analysis; elastic modulus.

INTRODUCTION

The success of dental implants is highly influenced by the biomechanical response at the implant-bone interface during occlusal load transfer (González-Mederos et al., 2025; Kriswanto et al., 2025; Sayed et al., 2025). Non-optimal distribution of stress and strain at the bone-implant interface can increase micromovement, bone resorption, and the risk of osseointegration failure (Ceddia et al., 2025; Falcinelli et al., 2023; González-Mederos et al., 2025). Thus, biomechanical evaluation plays an important role in optimizing implant design and assessing the long-term stability of the implant (Falcinelli et al., 2023; Sayed et al., 2025).

Finite element analysis (FEA) has been widely used to evaluate the distribution of stress, strain, and displacement in implant systems that are difficult to measure in vivo (Alemayehu et al., 2024; Chang et al., 2025; Sayed et al., 2025). This approach allows for the simulation of various loading conditions, bone quality, and geometric configurations in a controlled and reproducible manner (Afazal et al., 2025; Alemayehu et al., 2024; Chang et al., 2025). In implant biomechanics, the posterior mandibular model and the first molar bone block are often used to simulate clinical loading conditions in finite element analysis (Chang et al., 2025; Has & Orbak, 2025; Kriswanto et al., 2025).

Although FEA is widely used in implantology, most studies still assume bone as a homogeneous, isotropic, and linearly elastic material to simplify calculations (Alemayehu et al., 2024; Gasik et al., 2021; Li et al., 2025). This approach does not fully capture the mechanical behavior of bones because cortical and cancellous tissues exhibit direction-dependent responses to loading (Li et al., 2025; Marangon et al., 2025; Mathai et al., 2021). The orientation of trabecular cancellous bone and the microstructure of cortical bone cause different elastic responses in each loading direction (Marangon et al., 2025; Mathai et al., 2021). Therefore, the orthotropic approach is considered more representative than the isotropic model in biomechanical bone simulations (Li et al., 2025; Marangon et al., 2025; Mathai et al., 2021; Wang et al., 2024).

The mechanical properties of bones vary depending on factors such as density, microarchitecture, age, and the individual's biological and pathological conditions (Öhman-Mägi et al., 2021; Osterhoff et al., 2016; Zhang et al., 2023). Aging and decreased bone density are known to reduce bone stiffness, elastic modulus, and mechanical strength (Öhman-Mägi et al., 2021;

Osterhoff et al., 2016). The changes cause variations in the elastic modulus and shear modulus among individuals and bone conditions, so using a single material value has the potential to produce a less realistic biomechanical representation (Mathai et al., 2021; Öhman-Mägi et al., 2021; Zhang et al., 2023).

Several studies have reported that variations in bone material properties contribute to changes in stress and strain distributions and the primary stability of the implant system (Afazal et al., 2025; Ceddia et al., 2025; Vautrin et al., 2025). Although FEA studies on dental implants have extensively evaluated implant geometry, thread design, and loading conditions, modeling realistic variations in bone material properties has not yet been widely explored (Afazal et al., 2025; Alemayehu et al., 2024; Kriswanto et al., 2025). Furthermore, the influence of variations in bone material properties on the orthotropic model of cortical and cancellous bone has not yet been extensively evaluated in FEA studies (Hindurao et al., 2024; Mathai et al., 2021; Vautrin et al., 2025).

Sensitivity analysis is important for evaluating how variations in bone mechanical properties affect the biomechanical response of the implant system (Hindurao et al., 2024; Singh et al., 2025; Vautrin et al., 2025). Although the orthotropic model has been used in various biomechanical studies, independent evaluation of the elastic modulus (E) and the shear modulus (G) remains relatively limited (Li et al., 2025; Mathai et al., 2021; Singh et al., 2025). In fact, the elastic modulus relates to the stiffness of the material under axial loading, while the shear modulus contributes to the response to shear deformation and load transfer at the bone-implant interface (Mathai et al., 2021; Singh et al., 2025). Because the elastic modulus and shear modulus represent different mechanical responses, variations in these two parameters have the potential to influence the biomechanical sensitivity of the implant system (Singh et al., 2025; Vautrin et al., 2025).

Until now, limited research has evaluated the influence of variations in elastic modulus and shear modulus on the biomechanical response of the orthotropic bone model of the implant system (Hindurao et al., 2024; Mathai et al., 2021; Vautrin et al., 2025). As a result, the influence of biological variability in bone on the biomechanical stability of implant design remains poorly understood (Hindurao et al., 2024; Vautrin et al., 2025). These limitations are important because an ideal implant design needs to maintain biomechanical stability even when physiological changes occur in the mechanical properties of the bone (Ceddia et al., 2025; Falcinelli et al., 2023; Vautrin et al., 2025).

Based on the aforementioned issue, this research proposes an analytical framework based on nine structured variations to represent the physiological changes in the properties of orthotropic bone material. Variations of up to ±15% from the baseline value are used to represent potential changes in bone mechanical properties related to density and aging (Öhman-Mägi et al., 2021; Osterhoff et al., 2016; Zhang et al., 2023). This research specifically evaluates the biomechanical sensitivity of the implant system to gradual changes in the elastic modulus and shear modulus of orthotropic cortical and cancellous bone.

Unlike the conventional approach, which uses fixed material parameters, this research separates the effects of elastic modulus and shear modulus to identify the contribution of each to the biomechanical response of the implant system. This approach enables the assessment of the biomechanical robustness of implant design against variations in loading conditions and bone quality by analyzing stress distribution, strain, displacement, and micromotion at the implant-bone interface (Ceddia et al., 2025; Falcinelli et al., 2023; Vautrin et al., 2025).

This study aims to evaluate the sensitivity and biomechanical robustness of implant systems to physiological variations in elastic and shear moduli in cortical and cancellous orthotropic bone using finite element analysis. Specifically, this study assesses the distribution of stress, strain, and displacement as indicators of biomechanical stability and the potential success of osseointegration.

METHODS

A three-dimensional geometric model was developed as an idealized bone block representing the first mandibular molar region with a vertical dimension of 22 mm and a horizontal dimension of 20 mm. It consists of a homogeneous cortical bone layer with a thickness of 1.22 mm surrounding a cancellous bone core. This simplified configuration provides a standardized biomechanical model for evaluating the effects of variations in bone material properties on the biomechanical response of the implant–bone system, consistent with the virtual geometric modeling approach commonly adopted in finite element analysis. (Alqahtani et al., 2023; Ko et al., 2017). In this model, the implant system is represented as a three-component implant assembly consisting of a fixture, abutment, and fixation screw to simulate a two-piece implant configuration with an internal hexagonal connection. The fixture has a 5 mm diameter, a 10 mm length, and a reverse buttress thread profile, while the connection between the fixture and the abutment is stabilized with a fixation screw. All geometric models, including the bone block and implant assembly, were constructed using Autodesk Inventor Professional 2025. The schematic visualization of the finite element geometry used in this study is shown in Figure 1, which displays the dimensions of the bone block, implant configuration, and the arrangement of the implant assembly components that form the basis of the biomechanical simulation.

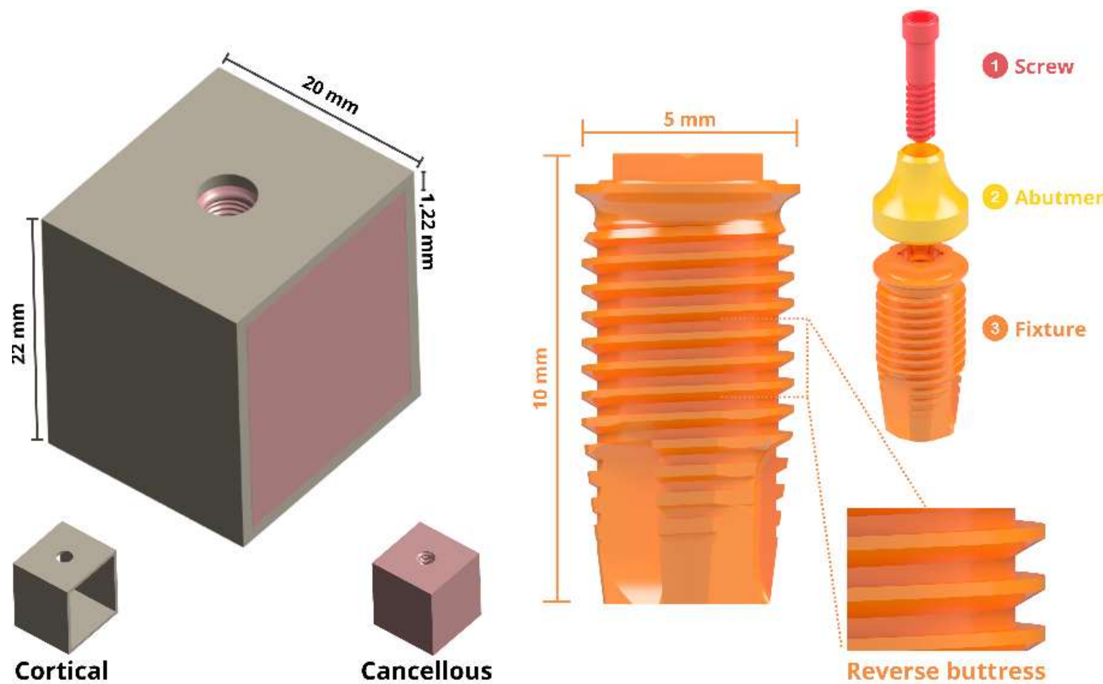

Figure 1. Schematic Geometry of the implant bone finite element model

Tabel 1. Baseline Orthotropic Material Properties of Cortical and Cancellous Bone

Component	Young's Modulus (GPa)	Shear Modulus (GPa)	Poisson's Ratio
Cortical Bone	*Ex* = 12.7 *Ey* = 22.8 *Ez* = 17.9	*Gxy* = 5.5 *Gyz* = 7.4 *Gxz* = 5.0	*vxy* = 0.31 *vyz* = 0.28 *vxz* = 0.18
Cancellous Bone	*Ex* = 0.511 *Ey* = 0.907 *Ez* = 0.114	*Gxy* = 0.434 *Gyz* = 0.081 *Gxz* = 0.078	*vxy* = 0.31 *vyz* = 0.30 *vxz* = 0.22
References: Ding et al. (2014)			

A finite element simulation was conducted using ANSYS Workbench 2023 R1 on a workstation with an Intel® Core™ i5-12500H processor and 32 GB of main memory. The implant assembly is modeled as an isotropic, homogeneous, and linear-elastic material using the Ti–6Al–4V (Grade 5) alloy, with an elastic modulus of 119 GPa and a Poisson's ratio of 0.37, adopted from material data available in (*AzoM*, n.d.) The orthotropic parameter material, which includes the elastic modulus, shear modulus, and Poisson's ratio in the main directions of the material, is obtained from (Ding et al., 2014) and summarized in Table 1.

The orthotropic material variation strategy is summarized in Table 2. The baseline orthotropic properties of cortical and cancellous bone were adopted from Ding et al. (2014), while nine simulation cases (V1–V9) were generated to evaluate the sensitivity of the implant–bone system to physiological variations in bone mechanical properties. In *V1–V7*, both the elastic modulus (*Ex, Ey, Ez*) and shear modulus (*Gxy, Gyz, Gxz*) were simultaneously varied from −15% to +15% relative to the baseline model. To independently evaluate the contribution of each orthotropic stiffness component, *V8* was generated by increasing only the elastic modulus while maintaining the baseline shear modulus, whereas *V9* was generated by increasing only the shear modulus while maintaining the baseline elastic modulus. Poisson's ratios remained unchanged throughout all simulation cases.

Table 2. Orthotropic Material Properties Assigned to Each Simulation Case

Component	Property	Gradual Variation							Independent Variation	
		V1 -15%	V2 -10%	V3 -5%	V4 0%	V5 +5%	V6 +10%	V7 +15%	V8 E↑	V9 G↑
Cortical Bone	Ex (GPa)	10.795	11.430	12.065	12.700	13.335	13.970	14.605	14.605	12.700
	Ey (GPa)	19.380	20.520	21.660	22.800	23.940	25.080	26.220	26.220	22.800
	Ez (GPa)	15.215	16.110	17.005	17.900	18.795	19.690	20.585	20.585	17.900
	Gxy (GPa)	4.675	4.950	5.225	5.500	5.775	6.050	6.325	5.500	6.325
	Gyz (GPa)	6.290	6.660	7.030	7.400	7.770	8.140	8.510	7.400	8.510
	Gxz (GPa)	4.250	4.500	4.750	5.000	5.250	5.500	5.750	5.000	5.750
Cancellous Bone	Ex (GPa)	0.434	0.460	0.485	0.511	0.537	0.562	0.588	0.588	0.511
	Ey (GPa)	0.771	0.816	0.861	0.907	0.952	0.998	1.043	1.043	0.907
	Ez (GPa)	0.097	0.103	0.108	0.114	0.120	0.125	0.131	0.131	0.114
	Gxy (GPa)	0.369	0.391	0.412	0.434	0.456	0.477	0.499	0.434	0.499
	Gyz (GPa)	0.069	0.073	0.077	0.081	0.085	0.089	0.093	0.081	0.093
	Gxz (GPa)	0.066	0.070	0.074	0.078	0.082	0.086	0.090	0.078	0.090

All interfaces between the fixture, abutment, screw, and bone tissue are modeled using fully bonded contact conditions to represent an ideal osseointegration state, with no relative slip at the contact interfaces. This assumption represents full biomechanical integration and does not account for partial bonding conditions or the initial healing phase. Physiological loading is applied to the occlusal surface of the abutment using three-dimensional force components based on in vivo data in the mandibular first molar region, which are -175.5 N in the Y direction, -5.8 N in the X direction, and -25.1 N in the Z direction (Bing et al., 2020). The boundary condition is set by applying a fully fixed constraint to the inferior bone block to prevent rigid body motion during the simulation. The physiological stiffness of the mandible in the region of interest is modeled through fixed support on the mesial and distal surfaces of the cortical and cancellous bone. The load configuration and boundary conditions are shown in Figure 2

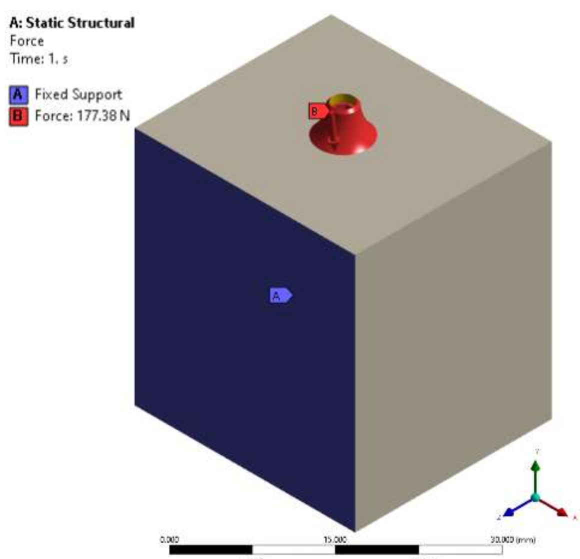

Figure 2. Finite element boundary conditions and physiological loading applied to the implant bone model with mesial distal fixed support.

Mesh convergence testing is performed before the simulation to verify the solution's independence of mesh density. The finite element model used three-dimensional tetrahedral elements with a global element size ranging from 5.0 to 4.3 mm. Local mesh refinement was applied at the implant–bone interface area through face sizing of 0.5 mm for cortical bone and 0.6 mm for cancellous bone (Figure 3). The mesh size variations produce models with 23.049–23.163 elements and 41.061–41.342 nodes. Convergence was evaluated using von Mises stress on the implant components (*σvmF, σvmS,* and *σvmA*) as well as maximum principal stress on cortical and cancellous bone (*σCt* and *σCn*). As shown in Table 3, successive mesh refinements within the global mesh size range of 4.7–4.5 mm produced variations below the 1% convergence criterion for all evaluated stress parameters, confirming that the numerical solution had reached mesh independence. Consequently, a global mesh size of 4.6 mm, comprising 23,134 elements and 41,251 nodes, was adopted for all subsequent simulations, as it ensures sufficient numerical accuracy while maintaining computational efficiency.

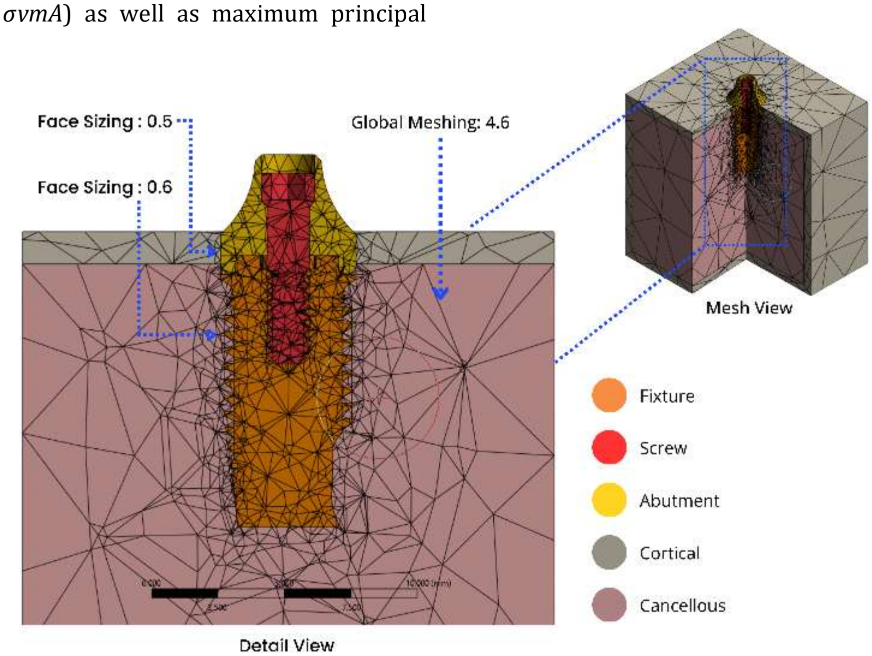

Figure 3. Finite element mesh distribution with global meshing and local face sizing around the implant bone interface.

Tabel 3. Mesh Convergence Analysis of Stress Predictions Across Successive Element Sizes

Global Mesh Size (mm)	$\sigma_{vm}F$	$\sigma_{vm}S$	$\sigma_{vm}A$	σCt	σCn
5.0 → 4.9	0.33%	1.53%	4.42%	13.55%	0.79%
4.9 → 4.8	-0.05%	0.18%	-0.19%	3.53%	-5.01%
4.8 → 4.7	0%	0%	0%	0%	0%
4.7 → 4.6	0%	0%	0%	0%	0%
4.6 → 4.5	0%	0%	0%	0%	0%
4.5 → 4.4	-0.24%	-1.15%	8.65%	-13.06%	-6.31%
4.4 → 4.3	-0.46%	0.02%	-10.11%	13.58%	-64.80%

Note: *σ* = *vm* Mises stress; *F* = fixture; *S* = screw; *A* = abutment; *Ct* = cortical bone; *Cn* = cancellous bone.

Biomechanical response of the implant system in bone evaluated using von Mises stress, principal stress, strain, and displacement on the implant components and peri-implant tissue (Falcinelli et al., 2023; Prados-Privado et al., 2020). The parameter is chosen to represent the stress distribution, load redistribution, and deformation response related to the biomechanical stability of the implant-bone system under physiological loading conditions (Falcinelli et al., 2023; Marangon et al., 2025).

A deterministic one-at-a-time (OAT) parametric sensitivity analysis was performed to quantify the influence of the orthotropic material variations defined in Table 2 on the biomechanical response of the implant–bone system. For the gradual orthotropic variations (*V1–V7*), the evaluation focused on von Mises stress on the screw and fixture, principal stress on the bone, cortical strain, and cortical displacement as the main indicators of biomechanical response. Furthermore, in the independent sensitivity evaluation between elastic modulus and shear modulus (*V8–V9*), screw stress, cortical principal stress, and cortical displacement were used as representative parameters to assess changes in stress distribution, peri-implant load transfer, and local deformation response (Ding et al., 2014; Marcián et al., 2018; Taheri et al., 2018).

Sensitivity of biomechanical response to material variations analyzed using relative percentage change (%Δ) and coefficient of variation (CV) (Hindurao et al., 2024; Vautrin et al., 2025).

$$\%\Delta = \frac{X_i - X_0}{X_0} \times 100$$

where Xi represents the biomechanical response value for each material variation, while X0 incates the response value on the baseline model. The coefficient of variation is used to evaluate the relative variability of the biomechanical response across all orthotropic material configurations and is calculated using Equation (2): gunakan Persamaan (2):

$$CV = \frac{\sigma}{\mu} \times 100$$

where σ denotes the standard deviation and μ represents the mean value of the evaluated biomechanical parameter. Lower CV values indicate lower variability of the biomechanical response across orthotropic material configurations

RESULTS AND DISCUSSION

3.1 Stress Distribution in the Implant–Bone System

Tabel 4. Maximum von Mises and Principal Stress Values for the Baseline Model

Output	Stress (Mpa)
σvmF	32.339
σvmS	41.381
σvmA	34.362
$\sigma 1Ct$	35.255
$\sigma 1Cn$	3.5275

The stress distribution on the baseline model shows the highest von Mises stress concentration at the implant–abutment and screw connection areas, especially around the internal hex connection and the cervical part of the implant (Figure 4). The screw shows a maximum stress value of 41.38 MPa, followed by the abutment at 34.36 MPa and the fixture at 32.34 MPa (Table 4). The stress concentration at the internal connection indicates that this area is a critical location for load accumulation during occlusal loading due to direct mechanical contact between implant assembly components

To verify the numerical model used, the maximum von Mises stress value on the implant assembly is compared with the results of a reference study that uses a comparable loading configuration and implant system. (Talmazov et al., 2020). The validation results show a difference of 0.9%, indicating a very good agreement between the developed model and the reference model. This finding supports the validity of the finite element model used as the basis for the sensitivity analysis of orthotropic material in this study.

The principal stress distribution shows that the cortical bone experiences a maximum stress of 35.26 MPa, localized in the crestal cortical region around the implant neck, while the cancellous bone only exhibits a stress of 3.53 MPa with a more dispersed distribution in the trabecular tissue (Figure 5). This pattern indicates that the cortical bone more predominantly supports physiological load transfer due to its higher elastic modulus compared to cancellous bone (Prados-Privado et al., 2020). This pattern may be associated with the substantially higher elastic modulus of cortical bone compared with cancellous bone, which influences load distribution within the implant–bone system (Ding et al., 2014; Nokar et al., 2020)

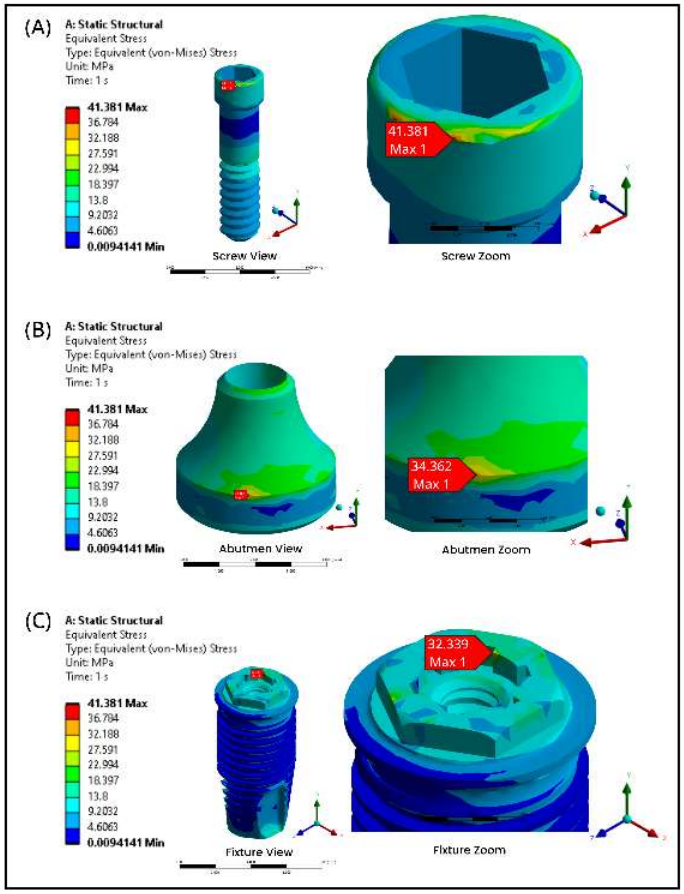

Figure 4. Von Mises stress distribution in the implant assembly for the baseline orthotropic model (V4)

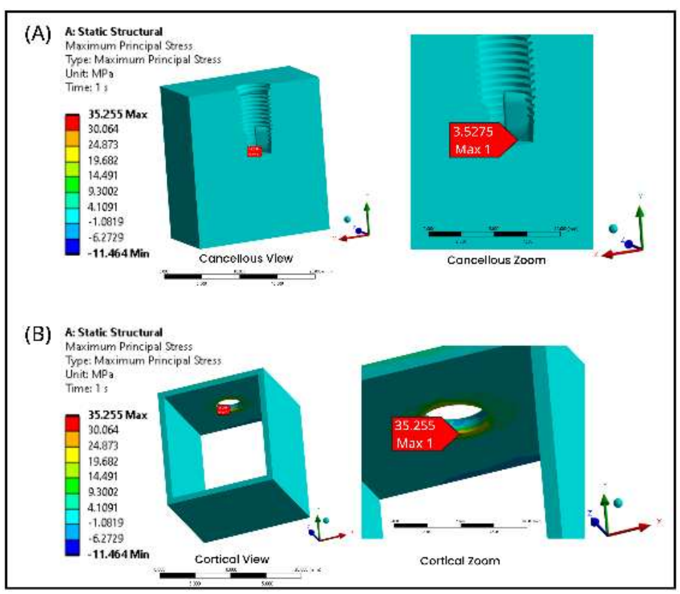

Figure 5. Maximum principal stress distribution in cortical and cancellous bone for the baseline orthotropic model (*V4*).

JPTM
http://journal.unnes.ac.id

3.2 Effect of Orthotropic Material Variation

Variations in the orthotropic material properties directly influence the biomechanical response of the implant–bone system, particularly through stress redistribution and interfacial deformation. Increasing the material stiffness from *V1* to *V7* gradually reduces screw stress (σvmS) from 42.06 MPa to 39.72 MPa, accompanied by a slight decrease in fixture stress (σvmF) from 32.20 MPa to 32.00 MPa. Conversely, the principal stress ($\sigma 1Ct$) in the cortical bone increases from 30.8 MPa to 36.8 MPa.

The pattern indicates that increasing directional stiffness shifts load transfer toward the crestal cortical bone around the implant neck. A stiffer orthotropic structure limits internal deformation in the trabecular area, causing stress concentrations to shift to the cortical bone. These findings are consistent with previous studies showing that orthotropic material representation alters stress distribution patterns and reduces localized stress concentrations relative to isotropic models (Ding et al., 2014).

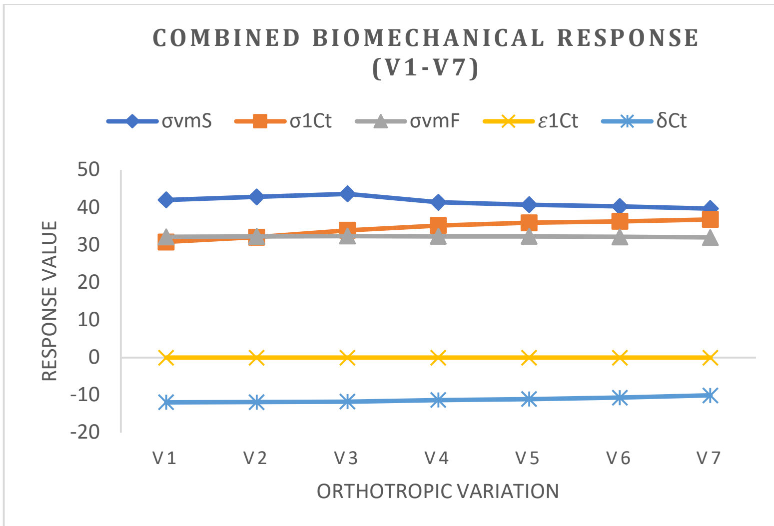

Figure 6. Combined biomechanical response of the implant–bone system under orthotropic material variations (V1–V7)

Changes in material stiffness also affect peri-implant deformation. Cortical strain ($\varepsilon 1Ct$) decreases from 0.00184 at V1 to 0.00152 at *V7,* while cortical displacement (δCt) decreases from −11.92 µm to −10.10 µm. The reduction in strain and displacement indicates an increase in the structural stiffness of the implant–bone system, thereby limiting local deformation during physiological loading. These findings suggest an increase in structural stiffness and a more stable mechanical response of the peri-implant during physiological loading. However, the increase in stiffness is also accompanied by increased stress on the crestal cortical bone, indicating a mechanical trade-off between reducing deformation and increasing local stress concentration. The peri-implant cortical bone, particularly in the crestal region surrounding the implant neck, exhibited the highest stress concentrations during functional loading (Ding et al., 2014; Nokar et al., 2020).

Biomechanical sensitivity analysis shows that an independent increase in elastic modulus (*V8*) raises screw stress to 43.2 MPa and cortical stress to 36.7 MPa compared with the baseline model (*V4*). In comparison, an increase in shear modulus (*V9*) decreases screw stress to 40.8 MPa and cortical stress to 34.0 MPa (Figure 7 and Table 5). These results indicate that the elastic modulus plays a dominant role in the overall stress distribution on the implant assembly. In contrast, the shear modulus has a greater influence on local deformation and interfacial stability at the implant–bone interface. The distinct biomechanical responses observed following independent variations in elastic modulus and shear modulus indicate that different orthotropic stiffness components contribute differently to stress redistribution and local deformation within the implant–bone system. This observation is consistent with previous studies showing that bone anisotropy and material stiffness influence stress distribution and load-transfer behaviour under physiological loading conditions (Raffa et al., 2021; Taheri et al., 2018).

Tabel 5. Comparative sensitivity analysis between elastic modulus and shear modulus variations.

Parameter	Baseline (V4)	Elastic Modulus (V8) E ↑	Shear Modulus (V9) G ↑
σvmS	41.381	43.2	40.8
$\sigma 1Ct$	35.255	36.7	34
δCt	-11.34	-10.97	-10.68

Note: σvmS, von Mises stress in the screw; σ1Ct, maximum principal stress in cortical bone; δCt, cortical bone displacement.

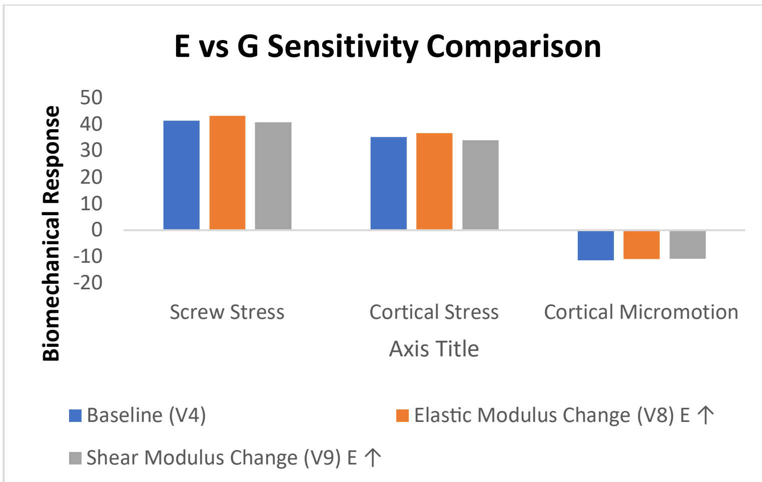

Figure 7. Comparative sensitivity between elastic modulus and shear modulus variations on biomechanical responses of the implant–bone system

3.3 Relative Percentage Change and Coefficient of Variation

The relative percentage change (%Δ) analysis shows that variations in orthotropic material properties result in different biomechanical sensitivities for each evaluation parameter (Figure 8). Deformation parameters, particularly cortical strain and displacement, exhibit greater relative changes than the stress distribution. Cortical strain in the cancellous region increased up to 18.55% at the −15% variation (*V1*) and decreased to −13.71% at the +15% variation (*V7*), while cortical displacement changed from 17.01% to −12.59% over the same variation range. Conversely, screw stress only showed a maximum deviation of 5.46% at *V1* and −4.02% at V7.

The results indicate that the deformation response is more sensitive to changes in directional stiffness than is the global stress distribution. The high sensitivity of strain and displacement suggests that changes in orthotropic mechanical properties heavily influence local deformation in the peri-implant area. Conversely, the stress response in the implant assembly tends to remain consistent compared to that in the peri-implant tissue, indicating that variations in orthotropic material properties primarily affect the local stress distribution in the bone rather than the overall response of the implant structure (Hindurao et al., 2024).

The evaluation of the coefficient of variation (*CV*) shows that the stress distribution parameters have relatively high numerical stability against variations in orthotropic material (Figure 9). The *CV* values for σvmF, σvmS, and σvmA are 0.37%, 3.05%, and 2.22%, respectively, while the principal stress in cortical and cancellous bone are recorded at 1.98% and 1.55%. Conversely, the deformation parameters exhibit higher variation, especially for $\varepsilon 1Ct$ at 9.63%, $\varepsilon 1Cn$ at 10.43%, δF at −9.60%, and δCt at −9.57%.

The higher coefficients of variation observed for strain and displacement indicate that deformation-related parameters are more responsive to orthotropic material variations than stress-based metrics within the present finite element model. This finding suggests that local deformation responses are particularly sensitive to changes in directional stiffness and may therefore provide a useful indicator for evaluating peri-implant biomechanical adaptation. Similar observations have been reported in studies emphasizing the influence of bone mechanical properties on local deformation patterns and implant stability (Marcián et al., 2018; Taheri et al., 2018)

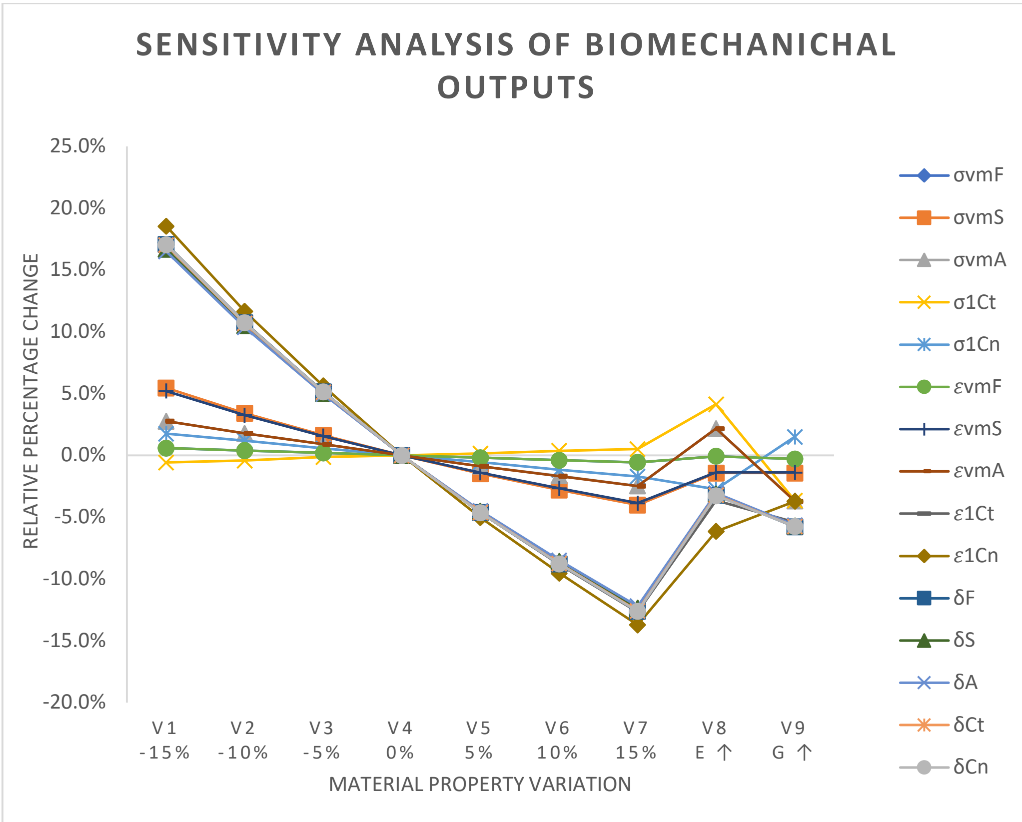

Figure 8. Sensitivity analysis of biomechanical outputs based on relative percentage change across orthotropic material property variations. Abbreviations: σvm, von Mises stress; σ1, principal stress; ε, strain; δ, displacement; F, fixture; S, screw; A, abutment; Ct, cortical bone; Cn, cancellous bone.

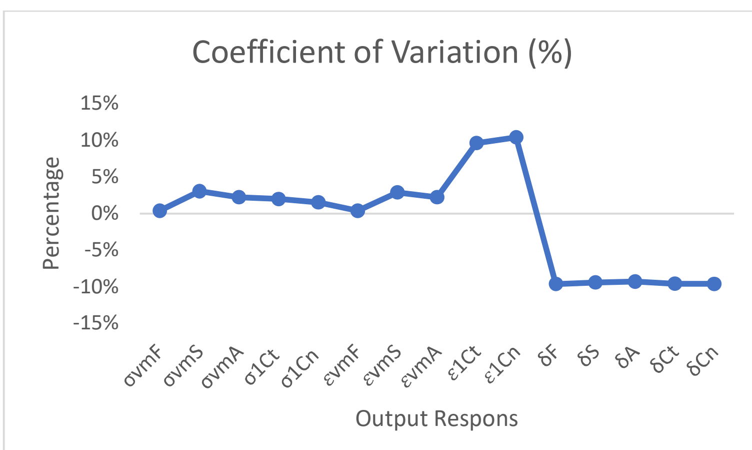

Figure 8. Coefficient of variation (CV) of biomechanical responses under orthotropic material variations

3.4 Comparison with Previous Studies and Limitations

The stress distribution pattern in this study shows a concentration of stress primarily in the crestal cortical bone area and the implant–abutment connection area. This finding is consistent with previous finite element studies that reported the crestal cortical bone as the primary load-transfer area during functional loading of implant-supported restorations, making it the location with the highest stress concentration around the implant (Nokar et al., 2020; Prados-Privado et al., 2020).

The increase in principal stress in cortical bone observed in this study indicates that changes in bone material properties affect load redistribution in the peri-implant tissue (Ding et al., 2014), which reports that representing bone as an orthotropic material results in different stress and strain distributions compared to an isotropic model and significantly influences the biomechanical response of the bone around the implant. In this study, increasing the material stiffness decreases the strain and displacement of cortical bone but simultaneously increases the principal stress in the peri-implant cortical area, indicating a trade-off between reducing local deformation and increasing stress concentration.

Sensitivity analysis shows that deformation parameters, particularly strain and displacement, experience greater relative changes compared to stress parameters when evaluating variations in material properties. The results of the relative percentage change and coefficient of variation indicate that the biomechanical response of the developed model is more sensitive to deformation parameters than to stress parameters. Additionally, increasing the elastic modulus independently results in greater increases in screw and cortical stress than increasing the shear modulus. In contrast, variations in shear modulus have a relatively smaller effect on the observed biomechanical response. These findings suggest that the elastic modulus is a more dominant material parameter influencing load redistribution in the implant–bone system within the model configuration used. Overall, these results are consistent with previous studies showing that changes in bone material properties and modeling assumptions can lead to different biomechanical responses in the implant–bone system (Hindurao et al., 2024; Vautrin et al., 2025).

Sensitivity analysis shows that deformation parameters, particularly strain and displacement, experience greater relative changes compared to stress parameters when evaluating variations in material properties. The results of the relative percentage change and coefficient of variation indicate that the biomechanical response of the developed model is more. This study has several limitations. The finite element model assumes homogeneous, linear-elastic material behavior and fully bonded contact conditions, which represent ideal osseointegration. Additionally, the simulation considers only physiological static loading, without accounting for cyclic loading, bone remodeling, or patient-specific anatomical variations. Therefore, the developed model does not fully represent the complexity of actual clinical conditions during long-term mastication function.

Nevertheless, the sensitivity analysis approach based on variations in elastic modulus and shear modulus in the orthotropic bone model used in this study provides a systematic framework for evaluating the influence of physiological variability in bone mechanical properties on the biomechanical response of the implant–bone system. Future research should integrate patient-specific geometry, nonlinear, anisotropic material behavior, fatigue-loading simulations, and bone-remodeling mechanisms to enhance the biomechanical and clinical relevance of finite element predictions.

CONCLUSIONS

This study demonstrated that physiological variations in the orthotropic mechanical properties of cortical and cancellous bone significantly influence the biomechanical response of a mandibular first molar implant system. Finite element sensitivity analysis showed that increasing orthotropic stiffness reduced peri-implant strain and displacement while increasing stress concentration in the crestal cortical bone, indicating a biomechanical trade-off between deformation reduction and local stress redistribution. Furthermore, independent sensitivity evaluation revealed that the elastic modulus primarily governs global stress distribution within the implant assembly, whereas the shear modulus has a greater influence on local deformation and peri-implant stability. Overall, these findings confirm that orthotropic material representation provides a more realistic assessment of implant biomechanics under physiological variations in bone properties and can improve the reliability of finite element analyses for evaluating implant biomechanical performance.

REFERENCE

Afazal, M., Afreen, S., & Chanda, A. (2025). Three-dimensional static finite element analysis for evaluating different implant–Abutment configurations in dental implants. *Next Bioengineering*, *1*, 100010. https://doi.org/https://doi.org/10.1016/j.nxbio.2025.100010

Alemayehu, D. B., Todoh, M., & Huang, S.-J. (2024). Advancing 3D Dental Implant Finite Element Analysis: Incorporating Biomimetic Trabecular Bone with Varied Pore Sizes in Voronoi Lattices. In *Journal of Functional Biomaterials* (Vol. 15, Number 4, p. 94). https://doi.org/10.3390/jfb15040094

AzoM. (n.d.). Retrieved June 11, 2026, from https://www.azom.com/properties.aspx?ArticleID=1547

Bing, L., Mito, T., Yoda, N., Sato, E., Shigemitsu, R., Han, J.-M., & Sasaki, K. (2020). Effect of peri-implant bone resorption on mechanical stress in the implant body: In vivo measured load-based finite element analysis. *Journal of Oral Rehabilitation*, *47*(12), 1566–1573. https://doi.org/10.1111/joor.13097

Ceddia, M., Romasco, T., Marchioli, G., Comuzzi, L., Cipollina, A., Piattelli, A., Lamberti, L., Di Pietro, N., & Trentadue, B. (2025). Finite Element Analysis of Implant Stability Quotient (ISQ) and Bone Stresses for Implant Inclinations of 0°, 15°, and 20°. *Materials (Basel, Switzerland)*, *18*(7). https://doi.org/10.3390/ma18071625

Chang, C.-L., Chen, J.-J., & Chen, C.-S. (2025). Using optimization approach to design dental implant in three types of bone quality-A finite element analysis. *Journal of Dental Sciences*, *20*(1), 126–136.

Ding, X., Liao, S.-H., Zhu, X.-H., & Wang, H.-M. (2014). Influence of orthotropy on biomechanics of peri-implant bone in complete mandible model with full dentition. *BioMed Research International*, *2014*, 709398. https://doi.org/10.1155/2014/709398

Falcinelli, C., Valente, F., Vasta, M., & Traini, T. (2023). Finite element analysis in implant dentistry: State of the art and future directions. *Dental Materials*, *39*(6), 539–556. https://doi.org/https://doi.org/10.1016/j.dental.2023.04.002

Gasik, M., Lambert, F., & Bacevic, M. (2021). Biomechanical Properties of Bone and Mucosa for Design and Application of Dental Implants. In *Materials* (Vol. 14, Number 11, p. 2845). https://doi.org/10.3390/ma14112845

González-Mederos, P., Rodríguez-Guerra, J., González, J. E., Picardo, A., & Torres, Y. (2025). A Finite Element Analysis of a New Dental Implant Design: The Influence of the Diameter, Length, and Material of an Implant on Its Biomechanical Behavior. In *Materials* (Vol. 18, Number 12, p. 2692). https://doi.org/10.3390/ma18122692

Has, L. C., & Orbak, R. (2025). Effect of Bone Quality, Implant Length, and Loading Timing on Stress Transmission in the Posterior Mandible: A Finite Element Analysis. *Bioengineering (Basel, Switzerland)*, *12*(8). https://doi.org/10.3390/bioengineering12080888

Hindurao, Bhargav, Gujare, Aditya, Jadhav, Harshavardhan, & Dhatrak, Pankaj. (2024). Evaluate the effect of bone density variation on stress distribution at the bone–implant interface using numerical analysis. *Proceedings of the Institution of Mechanical Engineers, Part H: Journal of Engineering in Medicine*, *238*(5), 463–470. https://doi.org/10.1177/09544119241240940

Kriswanto, K., Jamari, J., Andika, R., Bayuseno, A. P., Yusuf, A. A., & Ammarullah, M. I. (2025). Fixture design effects on posterior dental implant stability using finite element analysis (FEA): a systematic review. *Head & Face Medicine*, *22*(1), 2. https://doi.org/10.1186/s13005-025-00566-x

Li, Y.-C., Hwang, J.-R., Fung, C.-P., & Chung, C.-Y. (2025). Biomechanical Influence of Placement Angle and Loading Direction of Orthodontic Miniscrews on Orthotropic Mandible. In *Materials* (Vol. 18, Number 21, p. 4963). https://doi.org/10.3390/ma18214963

Marangon, G., Fincato, R., Carniel, E. L., Toniolo, I., Berardo, A., & Mazzucco, G. (2025). Orthotropic reconstruction and characterization of bone tissues through a visco-plasto-damage model. *PLOS ONE*, *20*(11), e0335948.

Marcián, P., Wolff, J., Horáčková, L., Kaiser, J., Zikmund, T., & Borák, L. (2018). Micro finite element analysis of dental implants under different loading conditions. *Computers in Biology and Medicine*, *96*, 157–165. https://doi.org/https://doi.org/10.1016/j.compbiomed.2018.03.012

Mathai, B., Dhara, S., & Gupta, S. (2021). Orthotropic bone remodelling around uncemented femoral implant: a comparison with isotropic formulation. *Biomechanics and Modeling in Mechanobiology*, *20*(3), 1115–1134. https://doi.org/10.1007/s10237-021-01436-6

Nokar, S., Jalali, H., Nozari, F., & Arshad, M. (2020). Finite Element Analysis of Stress in Bone and Abutment-Implant Interface under Static and Cyclic Loadings. *Frontiers in Dentistry*, *17*(21), 1–8. https://doi.org/10.18502/fid.v17i21.4315

Öhman-Mägi, C., Holub, O., Wu, D., Hall, R. M., & Persson, C. (2021). Density and mechanical properties of vertebral trabecular bone—A review. *JOR SPINE*, *4*(4), e1176. https://doi.org/https://doi.org/10.1002/jsp2.1176

Osterhoff, G., Morgan, E. F., Shefelbine, S. J., Karim, L., McNamara, L. M., & Augat, P. (2016). Bone mechanical properties and changes with osteoporosis. *Injury*, *47 Suppl 2*(Suppl 2), S11-20. https://doi.org/10.1016/S0020-1383(16)47003-8

Prados-Privado, M., Martínez-Martínez, C., Gehrke, S. A., & Prados-Frutos, J. C. (2020). Influence of Bone Definition and Finite Element Parameters in Bone and Dental Implants Stress: A Literature Review. *Biology*, *9*(8). https://doi.org/10.3390/biology9080224

Raffa, M. L., Nguyen, V.-H., Hernigou, P., Flouzat-Lachaniette, C.-H., & Haiat, G. (2021). Stress shielding at the bone-implant interface: Influence of surface roughness and of the bone-implant contact ratio. *Journal of Orthopaedic Research*, *39*(6), 1174–1183. https://doi.org/https://doi.org/10.1002/jor.24840

Sayed, A. J., Mohsin, S. F., Garg, K. K., Agwan, M. A. S., Tareen, S. U. K., Alruthea, M. S., & Mohan, S. (2025). Finite Element Analysis (FEA) for Influence of Variation in Dental Implant Dimensions (Length and Diameter) on Peri-implant Bone Stress/Strain Distribution: A Systematic Review. *Pakistan Journal of Medical Sciences*, *41*(1), 318–330. https://doi.org/10.12669/pjms.41.1.8991

Singh, R. K., Verma, K., Mohan Kumar, G. C., & Doddamani, S. (2025). Optimizing dental implant design parameters through orthotropic properties of bone: a DOE-based approach. *International Journal on Interactive Design and Manufacturing (IJIDeM)*, *19*(12), 8825–8837. https://doi.org/10.1007/s12008-025-02324-4

Taheri, R. A., Jarrahi, A., Farnoosh, G., & Karimi, A. (2018). A comparative finite element simulation of stress in dental implant–bone interface using isotropic and orthotropic material models in three mastication cycles. *Journal of the Brazilian Society of Mechanical Sciences and Engineering*, *40*(10), 489. https://doi.org/10.1007/s40430-018-1409-9

Talmazov, G., Veilleux, N., Abdulmajeed, A., & Bencharit, S. (2020). Finite element analysis of a one-piece zirconia implant in anterior single tooth implant applications. *PloS One*, *15*(2), e0229360. https://doi.org/10.1371/journal.pone.0229360

Vautrin, A., Zysset, P., & Varga, P. (2025). Influence of key modeling assumptions on the finite element prediction of dental implant primary stability. *Computers in Biology and Medicine*, *195*, 110587. https://doi.org/https://doi.org/10.1016/j.compbiomed.2025.110587

Wang, L., Meloro, C., Fagan, M. J., Kissane, R. W. P., Bates, K. T., Askew, G. N., & Watson, P. J. (2024). Regional variation of the cortical and trabecular bone material properties in the rabbit skull. *PloS One*, *19*(2), e0298621. https://doi.org/10.1371/journal.pone.0298621

Zhang, L., Guan, Q., Wang, Z., Feng, J., Zou, J., & Gao, B. (2023). Consequences of Aging on Bone. *Aging and Disease*, *15*(6), 2417–2452. https://doi.org/10.14336/AD.2023.1115